Qiu *et al. Carbon Research* (2023) 2:45
https://doi.org/10.1007/s44246-023-00079-9

Carbon Research

ORIGINAL ARTICLE

Open Access

Porous carbon material production from microwave-assisted pyrolysis of peanut shell

Tianhao Qiu[1†], Chengxiang Li[2†], Mengmeng Guang[1] and Yaning Zhang[1*]

Abstract

Due to the complex porous structure, biochar usually has good adsorption capacity. Therefore, compared with direct combustion, conversion of peanut shell into biochar by pyrolysis is considered to be an environmentally friendly and efficient method for agricultural solid waste disposal. In this study, biochar production from microwave-assisted pyrolysis of peanut shell was detailed. The yields, surface topographies, and pore structures (pore size distribution and micropore volume) of biochars prepared at different pyrolysis temperatures (700, 750, 800, 850, 900, and 950 °C), microwave powers (350, 400, 450, 500, and 550 W), and residence times (0.5, 1.0, 1.5, 2.0, and 3.0 h) were elaborated. The results showed that the biochar yield gradually decreased and finally stabilized to around 30% while the specific surface area improved within the range of 4.68–67.29 m^2/g when the pyrolysis temperature, microwave power, or residence time increased. Biochar with micropore was first obtained at pyrolysis temperature of 800 °C, microwave power of 500 W, and residence time of 2.0 h. This study further proposed quantitative relationships between the pore structures of peanut shell based biochars and experimental conditions (pyrolysis temperature, microwave power and residence time). The results presented in this study can provide guidance for the reuse of peanut shell and the production of porous biochar. The peanut shell biochar prepared in this study can be used in soil remediation, air purification, liquid purification and other fields for its porous structural characteristics.

Highlights

- Peanut shell based biochar was produced using microwave-assisted pyrolysis.
- Effects of pyrolysis operating parameters, such as pyrolysis temperature, microwave power, and residence time on the biochar yields, surface topographies, and pore structures were detailed.
- The biochar yields were in the range of 30.04–43.38 wt. %.
- The maximum specific surface area was 67.29 m^2/g at 950 °C, 500 W, and 2.0 h.

[†]Tianhao Qiu and Chengxiang Li are co-first authors and contributed equally to this work.

Handling Editor by Fengchang Wu.

*Correspondence:
Yaning Zhang
ynzhang@hit.edu.cn
Full list of author information is available at the end of the article

• Biochar with micropore appeared at pyrolysis temperature of 800 °C, microwave power of 500 W, and residence time of 2.0 h for the first time.

• Quantitative relationships between the pore structures of peanut shell based biochars and experimental conditions were proposed.

Keywords Microwave-assisted pyrolysis, Peanut shell, Biochar, Yield, Pore structure

Graphical Abstract

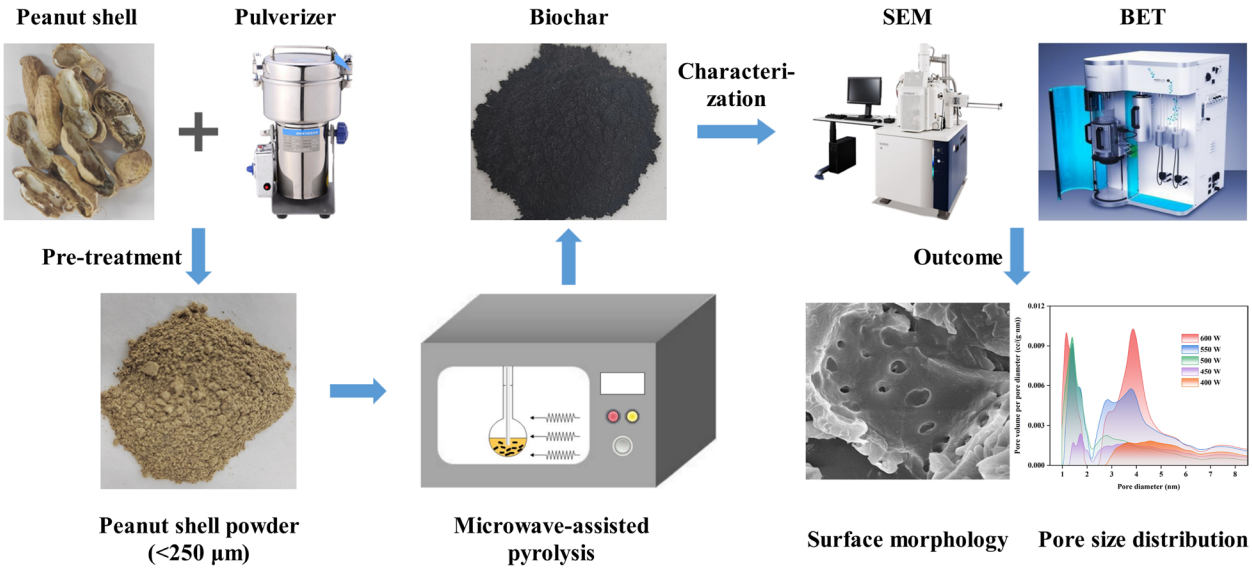

1 Introduction

Peanut shell is the by-product of peanut production. More than 4.0×10^7 t peanuts were produced in the world per year and increased at the rate of 1.16 million tons/year (Liu et al. 2018). Therefore, quantities of peanut shells were produced and most of them were discarded as solid waste or burned off, resulting in resource loss and environmental pollution (Cheng et al. 2016). Thus, it is of great importance to find new ways of comprehensive utilization of peanut shell. Nowadays, the conversion of peanut shell into biochar by pyrolysis is considered to be an environmentally friendly and efficient method for agricultural solid waste disposal (Fodah and Abdelwahab 2022; Fodah et al. 2020). Preparation of porous biochar has become a research hotspot (Fodah et al. 2020a). Biochar refers to carbon-rich material produced by thermal decomposition of organic raw materials under an anoxic or anaerobic atmosphere (Deng et al. 2020; Fodah and Ghosal 2021). In recent years, biochar has received increasing attention because of the properties of high porosity, large specific surface area, abundant functional group, and high electrical conductivity. Biochar produced from agricultural residues showed a great potential as biofuel (Fodah et al. 2021), soil remediation (Novak et al. 2019; Chen 2019; Chen et al. 2019), heavy metal adsorbent (Liu et al. 2022a; Huang et al. 2019; Kumuduni Niroshika Palansooriya et al. 2019), purification (Liu et al. 2020; Dissanayake et al. 2020), catalyst field (Zhang et al. 2020a), and electrochemical field (Sun et al. 2020; Amen et al. 2020; Motasemi et al. 2015), as shown in Fig. 1.

The pore structure properties of biochars are strongly controlled by the type of feedstock and the pyrolysis condition (Fodah et al. 2020b; Wei et al. 2020; Qiuhao et al. 2019) (such as pyrolysis method, pyrolysis temperature, heating rate, and residence time). Liu et al. (2018) studied the influences of pyrolysis conditions (pyrolysis temperature, retention time, heating rate, gas flow rate, and feedstock particle size) on the physical–chemical characteristics of biochar produced from peanut shell in a fixed-bed reactor. The results showed that the temperature played a major role in regulating the yields, distributions, and characteristics of biochars. Shan et al. (2020) studied the effect of temperature on the adsorption capacities of peanut shell based biochar

Fig. 1 Applications of porous biochar

and found that monolayer adsorption and chemical adsorption occupied an important role. Fan et al. (2022) studied the adsorption properties of diethyl phthalate by biochar samples produced from peanut shell at 300 ~ 800 °C, and the biochar produced at 800 °C had the highest specific surface area. Actually, most of the researches focused on traditional electric heating, which uses tube furnace or muffle furnace to pyrolysis peanut shells. During the electrical pyrolysis process, heat is transferred to the materials through convection heat transfer, radiation heat transfer and heat conduction, and the temperature is increased from the outside to the inside (Zhang et al. 2017a). Compared with electrical pyrolysis, microwave-assisted pyrolysis has been paid more and more attention by scholars because of the advantages of high conversion efficiency (Zhang et al. 2020b), low energy consumption (Zhang et al. 2017b), and uniform internal heating distribution (Ke et al. 2019) for biomass pyrolysis. These advantages are determined by its unique heating principle: the microwave radiation will cause the collision among the polar molecules inside the material, which directly converts the electromagnetic energy into the internal energy, making the temperature inside the material far higher than the external surface. Thus, the materials can be heat up rapidly and uniformly (Wang et al. 2020a). At present, there were a few studies on the adsorption properties of peanut shell based biochar prepared by microwave-assisted pyrolysis. For example, Chu et al. (2017) compared the pore properties of peanut shell biochars produced using microwave and muffle furnace. At the same pyrolysis temperature, biochar prepared by microwave-assisted pyrolysis preserved more biomass and had a larger surface area. However, only three sets of experimental results (200, 400, and 600 °C) were given. Fan et al. (2023) focused on the yields and higher heating values of the peanut shell based biochar. The highest biochar yield (86.0 wt. %) was obtained at 400 °C, 350 W, and 10 min. However, the pore structure properties of biochar were not studied.

Since there were no systematic studies on the microwave-assisted pyrolysis process of peanut shell under different pyrolysis conditions and the effects of pyrolysis conditions on the yield and pore structure of biochar up to now, the influences of pyrolysis operating parameters such as pyrolysis temperature, microwave power, and residence time on the yield, surface topography, and pore structures (pore size distribution and micropore volume) of peanut shell based biochars produced by microwave pyrolysis had been explored for the first time here.

2 Materials and methods

2.1 Materials

In this study, peanut shell from Henan Province (China) was chosen as the raw material. These peanut shells were first cleaned and oven-dried at 60 °C. Then they were crushed using a pulverizer and screened with a 60-mesh screen. The proximate analysis and ultimate analysis of these treated raw materials were done before the pyrolysis experiments, and the results were shown in Table 1. The result of ultimate analysis showed that carbon, hydrogen, nitrogen, oxygen, and sulfur accounted for 44.86%, 6.70%, 1.77%, 46.44%, and 0.23%, respectively. The result of proximate analysis showed that moisture, ash, volatile, and fixed carbon accounted for 5.40%, 4.81%, 69.89%, and 19.90% as percent of dry feedstock, respectively. In this study, the microwave absorbent was silicon carbide (SiC) with the density of 3230 kg/m^3 and the size of ~ 2 mm, which is inexpensive and easy to obtain.

2.2 Experimental setup

Three influencing factors (pyrolysis temperature, microwave power, and residence time) were studied here. It was found that the micropore of biochar showed at the pyrolysis temperature of 800 °C, the microwave power of 500 W, and the residence time of 2.0 h by preliminary experiments. Therefore, the operating conditions were designed as follows: (1) pyrolysis temperature (700, 750, 800, 850, 900, and 950 °C), (2) microwave power (400, 450, 500, 550, and 600 W), (3) residence time (1.0, 1.5, 2.0, 2.5, and 3.0 h), as shown in Table 2. In the preliminary experiment, we also found that when the mass ratio of peanut shell to SiC met 5:4, raw materials could rise to the pyrolysis temperature to be studied at the appropriate time. Through the preliminary experiment, other conditions like mass of peanut shell and SiC and volume of reactor were determined, which are shown in Table 3.

Table 1 Proximate analysis and ultimate analysis of peanut shell

Item	Value
Proximate analysis (wt. %)	
Moisture	5.40 ± 0.51
Ash	4.81 ± 0.23
Volatile	69.89 ± 1.06
Fixed carbon	19.90 ± 1.80
Ultimate analysis (wt. %)	
C	44.86
H	6.70
O	46.44
N	1.77
S	0.23

Table 2 Factors and conditions

Factor	Working condition
Pyrolysis temperature (°C)	700, 750, 800, 850, 900, 950
Residence time (h)	1.0, 1.5, 2.0, 2.5, 3.0
Microwave power (W)	400, 450, 500, 550, 600

Table 3 Other conditions in experiments

Parameter	Working condition
Particle size of peanut shell	< 250 μm
Mass of peanut shell	15 g
Mass of absorbent (SiC)	12 g
Reactor volume	50 ml

2.3 Experimental procedures

Figure 2 shows the schematic diagram of a microwave pyrolysis system established in a small laboratory setting in Harbin (China). The system consisted of five parts which included 11 kinds of facilities. Two K-type thermocouples (the temperature range was 0–1000 °C and the accuracy was 0.1 °C) were used to measure the biomass temperature here.

The specific experimental process of this work is shown below: (a) a quartz reactor was weighed and recorded. (b) 15 g peanut shell and 12 g SiC were mixed. (c) The microwave-assisted pyrolysis experimental system was connected. (d) The vacuum pump was turned on for about 10 min to create a vacuum atmosphere. (e) The microwave oven was turned on to start heating. When the microwave-assisted pyrolysis was over, the quartz reactor was reweighed. The difference between the quartz reactor before and after the experiment was biochar production. Each experiment was repeated three times to reduce the experimental errors.

2.4 Characterization

The surface topographies of biochar were observed by a scanning electron microscopy (SEM, VEGA3 LM, TESCAN, Czech). Adsorption–desorption isotherms of biochars were obtained by a volumetric gas adsorption instrument (Autosorb-iQ, Quantachrome Instruments, USA). The test was conducted in 77 K nitrogen atmosphere, and the sample was degassed at 250 °C for 12 h before the test. Based on the isothermal adsorption curve of adsorbed gas capacity with relative pressure, the Brunauer–Emmett–Teller (BET) method was used to analyze the specific surface area. The Density Functional Theory (DFT) method was used to analyze the pore size distribution and micropore volume. The microscopic properties of isotherm and adsorbent-adsorbent system were established by DFT through molecular statistical thermodynamic equations.

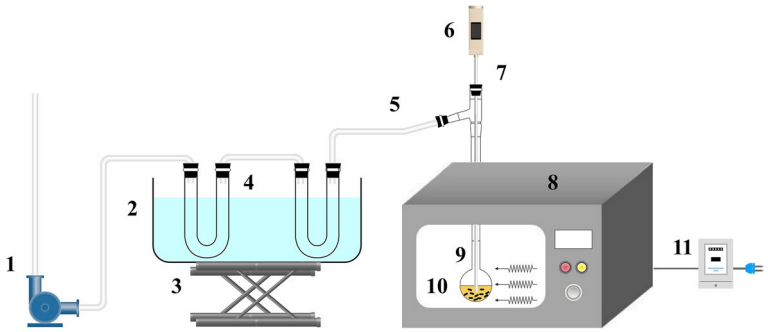

Fig. 2 Schematic diagram of experimental microwave-assisted pyrolysis system: (1) vacuum pump, (2) water tank, (3) bracket, (4) condenser, (5) pipe, (6) temperature sensor, (7) K-type thermocouple, (8) microwave oven, (9) quartz reactor, (10) insulation cotton, (11) electric meter

3 Results and discussion

3.1 Effect of pyrolysis temperature

In order to study the effect of pyrolysis temperature, six experiments (700, 750, 800, 850, 900, and 950 °C) were conducted at a fixed residence time and microwave power (2.0 h and 500 W, respectively).

3.1.1 Yield

Figure 3 shows the peanut shell based biochar yields obtained under different temperatures. The biochar yields were all gradually decreased from 31.11 wt. % to 30.04 wt. % with the increase of the pyrolysis temperature. This may be largely caused by the fact that more volatile compounds were released at higher pyrolysis temperatures and the secondary decomposition of biochar was also promoted (Chutia et al. 2014; Ippolito et al. 2021; Reza et al. 2020; Ghodszad et al. 2021; Liu et al. 2022b).

This study further used a parabola equation to describe the function correlation between yield Y and pyrolysis temperature T:

$$Y = 108.61 - 0.15T + (7.13E - 5)T^2 2(R^2 = 0.999) \quad (1)$$

where:

Y is the biochar yield, wt. %

T is the pyrolysis temperature, °C.

3.1.2 Surface topography

Many studies have proven that biochar is a porous material (Zhang et al. 2020c; Açma et al. 2001; Ahmad et al. 2014). The structure and morphology of biochar produced by the microwave-assisted pyrolysis of peanut shell under different temperatures (700, 750, 800, 900, and 950 °C) are shown in Fig. 4. The extent of devolatilization had significant influence on the characteristics of

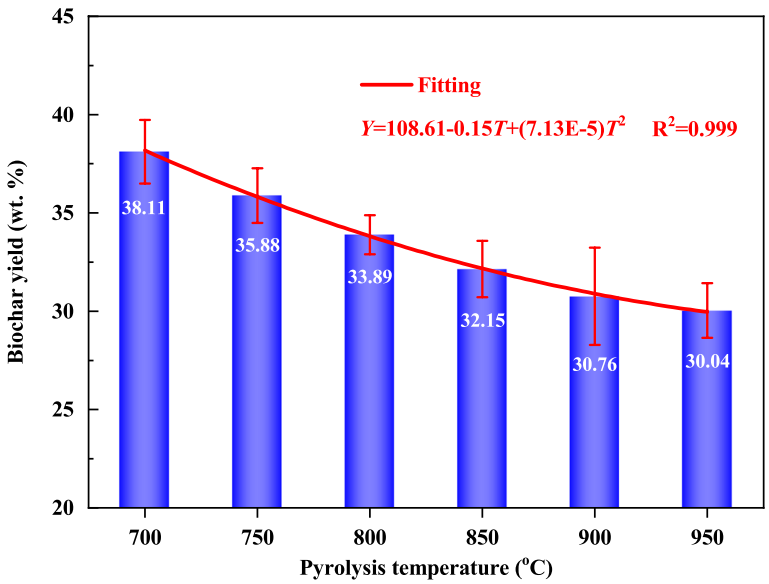

Fig. 3 Biochar yields at different pyrolysis temperatures

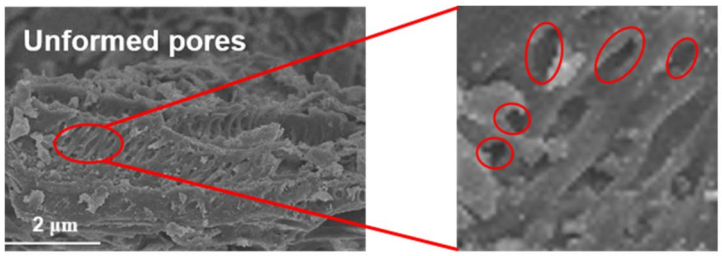

(a) 700 ºC

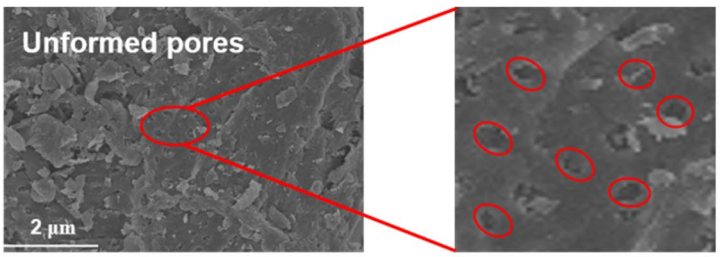

(b) 750 ºC

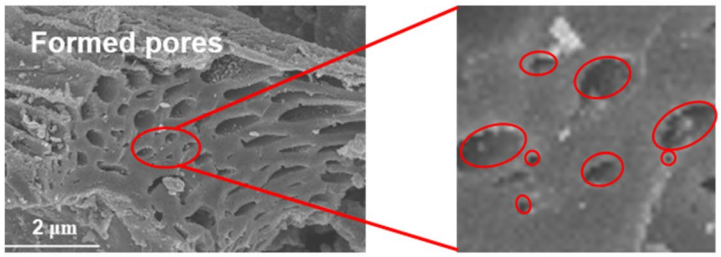

(c) 800 ºC

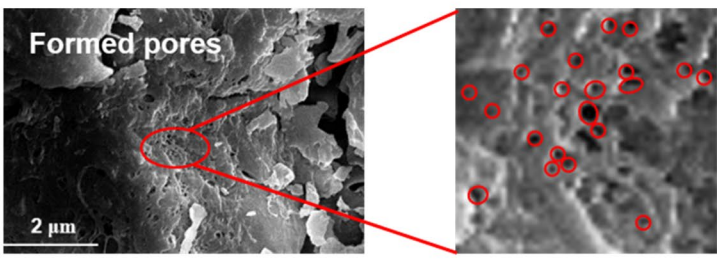

(d) 900 ºC

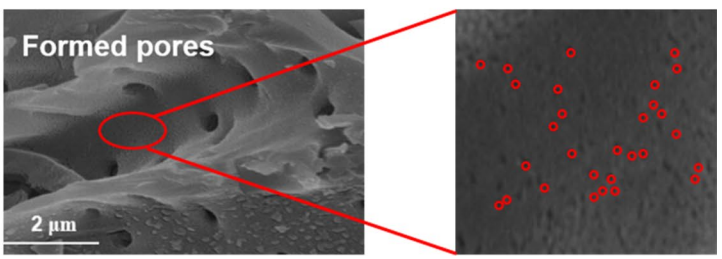

(e) 950 ºC

Fig. 4 SEMs of biochars at different pyrolysis temperatures. **a** 700 °C, **b** 750 °C, **c** 800 °C, **d** 900 °C, **e** 950 °C

biochar. As it is well known, the higher the volatile substances released, the lower the density of biochar, and the higher the porosity. As a result, different pore structures were formed (Açma et al. 2001; Ahmad et al. 2014; Antonangelo et al. 2019). As shown in Fig. 4 (a) and (b), when the pyrolysis temperature was 700 °C or 750 °C, most of the pores were unformed. As pyrolysis temperature increased, more volatile substances were released and at the same time more organic matters such as lignin and cellulose were broken down. Therefore, it can be seen in Fig. 4 (c), (d) and (e) that the pore sizes were decreased and the porosities and pore densities were increased as the temperature increased. In addition, the biochar was observed to have an unordered honeycomb structure. In particular, the crumpled structure of the biochar in Fig. 4 (d) can be caused by the broken-down of cellulose and lignin (Chen et al. 2011).

3.1.3 Pore size distribution

It can be seen from SEM images in Fig. 4 (c), (d), and (e) that biochar exhibited the preliminary porous structure, on which the effect of pyrolysis temperature was highly significant. Biochar obtained at 950 °C possessed a higher porosity than the biochar obtained at 800 °C (Fig. 4 (c) and (e)). Therefore, pore structure properties of the produced biochars were further illustrated by N_2 adsorption–desorption isotherms and the DFT method was used to analyze the pore size distribution in the range of 1 ~ 8 nm and the results are shown in Fig. 5.

It could be seen that when the pyrolysis temperature was below 800 °C, there were almost no micropores (< 2 nm) in the biochar; When the temperature exceeded 800 °C, the pore volumes of micropores increased gradually with the increase of temperature and the biochar produced at 950 °C contained more micropores, which reached 0.05 cc/(g·nm). This was because that some of the organic matter in peanut shell could be decomposed at relatively higher temperature thereby producing abundant pores (Li et al. 2020; Qiao et al. 2021; Nguyen et al. 2021).

3.1.4 Pore structure parameters

Figure 6 shows the micropore volumes of peanut shell based biochars obtained at different pyrolysis temperatures. The micropore did not appear until the pyrolysis temperature reached 800 °C, and with the temperature increased from 800 °C to 950 °C, the micropore volume increased continuously from 0.003 cc/g to 0.03 cc/g. At low temperatures, the pores were clogged with condensed organic matters (Jung et al. 2015; Zhang et al. 2021; Wang et al. 2020b). As the pyrolysis temperature increased, more volatiles were released, and the aliphatic alkyl and ester groups were continuously destroyed, forming voids in the biochar matrix (Liu et al. 2018; Özçimen and Ersoy-Meriçboyu 2010), which increased the formed pores and thereby increasing micropore volumes (Zhang et al. 2013; Bornemann et al. 2007).

In this study, a cubic equation was given to represent the function correlation between the micropore volume V_{micro} and pyrolysis temperature T:

$$V_{micro} = -6981 + 25.05T - 0.03T^2 + (1.2E-5)T^3 (R2 = 0.999) \quad (2)$$

where:

V_{micro} is the micropore volume, cc/g.

3.2 Effect of microwave power

In order to study the effect of microwave power, five experiments (400, 450, 500, 550, and 600 W) were conducted at a fixed residence time and pyrolysis temperature (2.0 h and 800 °C, respectively).

3.2.1 Yield

Figure 7 shows the peanut shell based biochar yields obtained at different microwave powers (400, 450, 500, 550, and 600 W). When the microwave power increased from 400 to 600 W, the biochar yields decreased from 39.67 wt. % to 32.12 wt. %. This was because that high microwave power accelerated the heating rate. The higher heating rate resulted in the rapid thermal degradation of lignocellulosic structures in peanut shell to primary volatiles, increasing the gaseous and liquid yield and limiting the possibility of formation of the biochar, which ultimately reduced the biochar yield (Manoj Tripathi and Sahu 2016; Demiral et al. 2012). The lower heating rate reduced the secondary reactions and cracking reactions, resulting in more biochar being produced (Demiral et al. 2012). Additionally, there would be local hot spots and uniform heat distribution in the peanut shell when the microwave power was high, resulting in a decline in biochar yield (Ping et al. 2019; Tayibi et al. 2019).

This study further used a parabola equation to describe the function correlation between biochar yield Y and microwave power P:

$$Y = 98.74 - 0.22P + (1.80E-4)P^2 (R^2 = 0.985) \quad (3)$$

where:

P is the microwave power, W.

3.2.2 Surface topography

Figure 8 shows the SEM images of peanut shell based biochars obtained at different microwave powers (400, 450, 500, 550, and 600 W). As shown in Fig. 8 (a) and (b), when the microwave power was 400 W or 450 W, most of the pores were unformed. As the microwave power

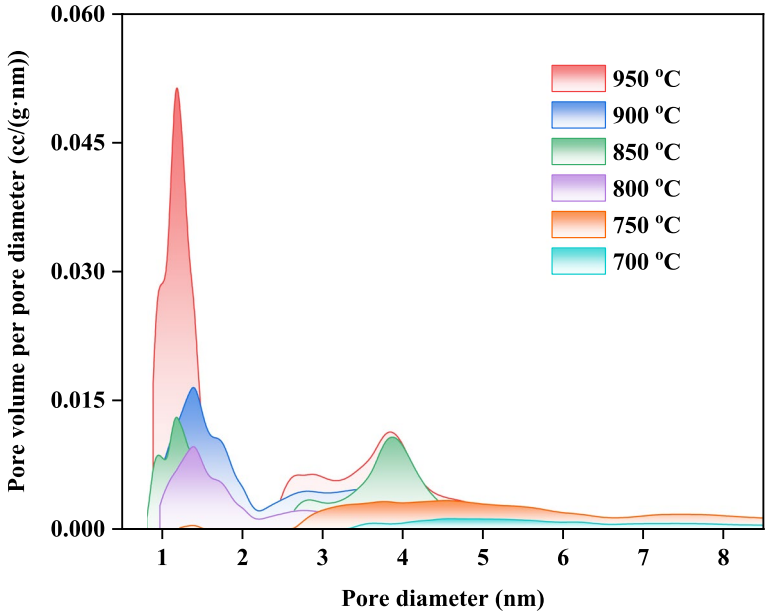

Fig. 5 Pore size distributions of biochars at different pyrolysis temperatures

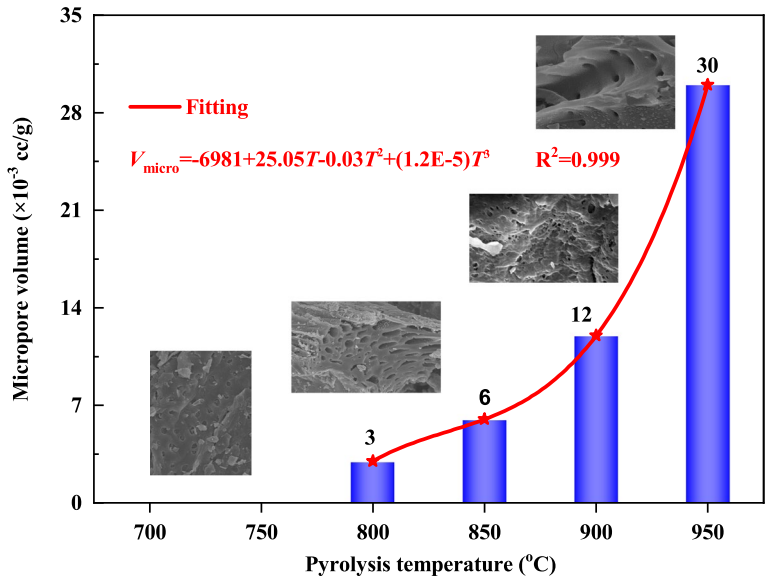

Fig. 6 Micropore volumes of biochars at different pyrolysis temperatures

increased, more volatile substances were released and more organic matters such as lignin and cellulose were broken down. Therefore, it can be seen in Fig. 8 (c), (d) and (e) that the pore sizes decreased and porosity and pore densities were increased with a bigger microwave power. Figure 8 (c) gives the surface topography of biochar prepared under 500 W. The surface was relatively rough and the pore size varied in the micrometer scale. There were many macropores and mesopores, which were interconnected and arranged irregularly. Figure 8 (e) shows the SEM image of biochar prepared under 600 W. It could be seen that compared with the biochar produced under 400–550 W, the number of pores with smaller aperture porosity was increased significantly.

3.2.3 Pore size distribution

It can be seen from SEM images in Fig. 8 (c), (d), and (e) that biochar exhibited the preliminary porous

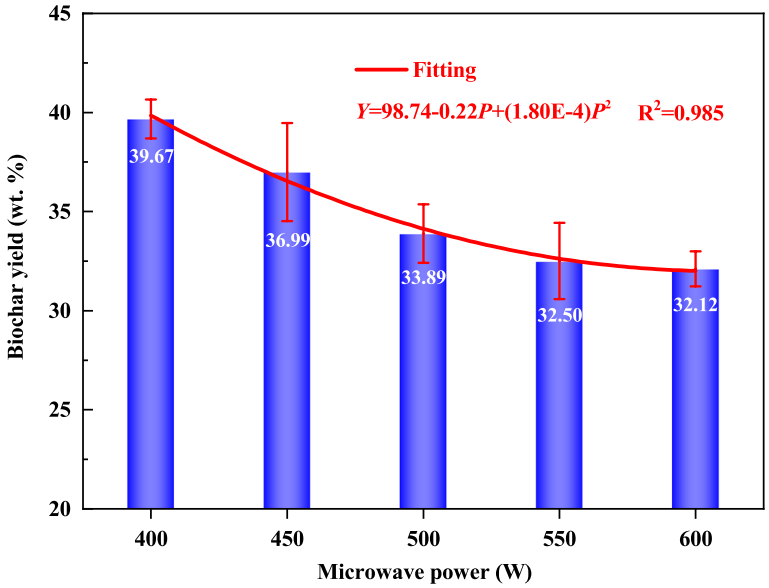

Fig. 7 Biochar yields at different microwave powers

structure, on which the effect of microwave power was highly significant. Biochar obtained at 600 W possessed a higher porosity than the biochar obtained at 500 W (Fig. 8 (c) and (e)). Therefore, pore structure properties of the produced biochars were further illustrated by N_2 adsorption–desorption isotherms. The DFT method was used to analyze the pore size distribution in the range of 1 ~ 8 nm and the results are shown in Fig. 9. It can be seen that when the microwave power was 400 W, there were almost no micropores (< 2 nm) in the biochar; when the microwave power exceeded 400 W, the pore volumes of micropores increased gradually with the increase of power. It was interesting that when the microwave power increased from 450 to 500 W, the number of pores in the range of 1 ~ 2 nm increased and when the power continued to increase to 600 W, the number of 3 ~ 4 nm pores increased.

3.2.4 Pore structure parameters

Figure 10 shows the msicropore volumes of peanut shell based biochars produced at different microwave powers (400, 450, 500, 550, and 600 W). The micropore did not appear until the microwave power reached 500 W, and the micropore volume increased persistently from 0.003 cc/g to 0.008 cc/g when the microwave power grown in the range of 500 W to 600 W. The higher the microwave power, the larger the pore volume, which was caused by the fracture caused by the destruction of the biochar structure (Tripathi et al. 2016). In fact, microwave power affected the heating rate by changing the microwave density in the microwave cavity (Motasemi and Afzal 2013; Arpiaa et al. 2021; Zhang et al. 2022). Higher microwave density meant that peanut shell could obtain more microwave energy and thus reach higher temperatures. Therefore, more volatiles were released and a higher micropore volume was obtained.

This study further used a parabola equation to describe the function correlation between the micropore volume V_{micro} and microwave power P:

$$V_{micro} = -38 - 0.17P + (2E-4)P^2 (R^2 = 0.999) \quad (4)$$

3.3 Effect of residence time

In order to study the effect of residence time, five experiments (1.0, 1.5, 2.0, 2.5, and 3.0 h) were conducted at a fixed pyrolysis temperature and microwave power (800 °C and 500 W, respectively).

3.3.1 Yield

Figure 11 shows the peanut shell based biochar yields produced at different residence times (1.0, 1.5, 2.0, 2.5, and 3.0 h). When the residence time increased from 1.0 h to 3.0 h, the biochar yield decreased from 43.28 wt. % to 33.62 wt. %, and this was largely due to that a longer residence time led to further breakdown of biochar, resulting in more release of volatile substances (Chen et al. 2003).

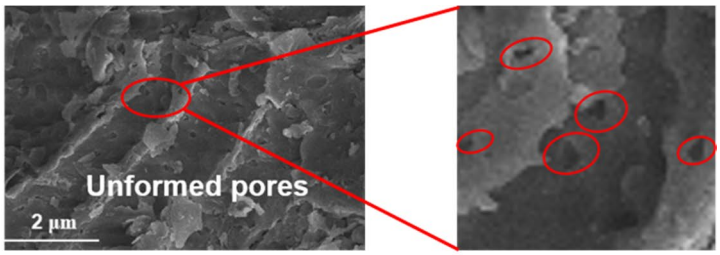

(a) 400 W

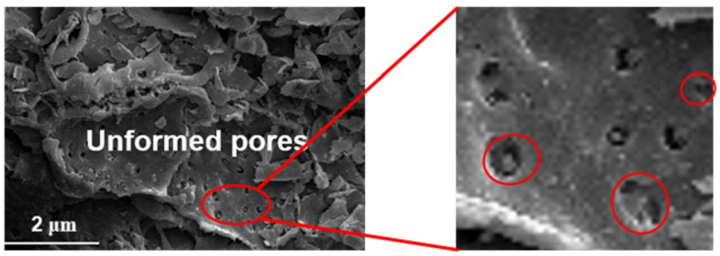

(b) 450 W

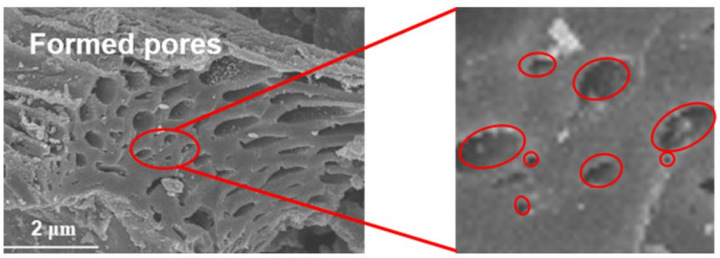

(c) 500 W

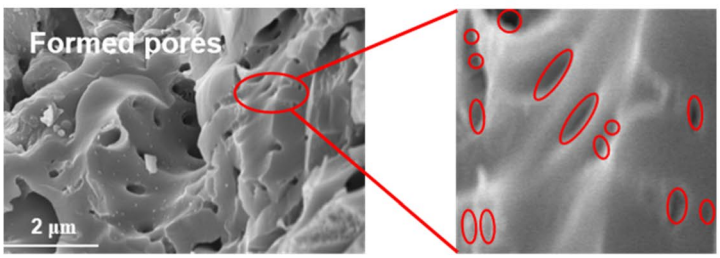

(d) 550 W

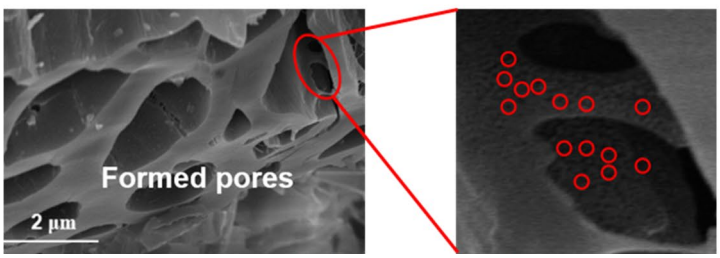

(e) 600 W

Fig. 8 SEMs of biochars at different microwave powers. **a** 400 W, **b** 450 W, **c** 500 W, **d** 550 W, **e** 600 W

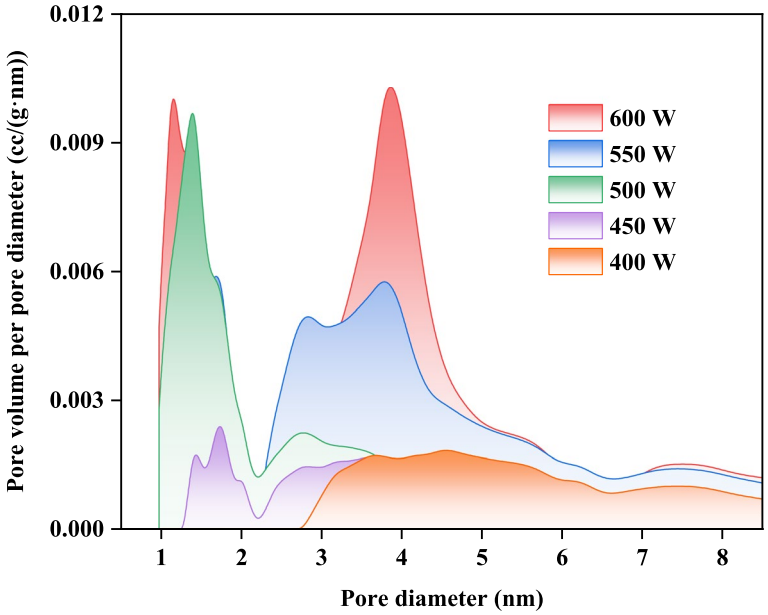

Fig. 9 Pore size distributions of biochars at different microwave powers

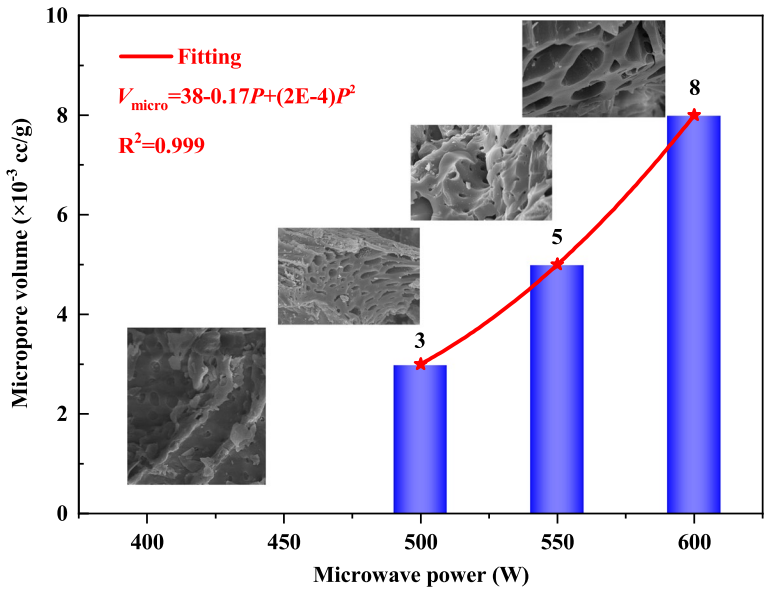

Fig. 10 Micropore volumes of biochars at different microwave powers

This study further used a parabola equation to describe the function correlation between yield Y and residence time t:

$$Y = 61.36 - 22.80t + 4.54t^2 (R^2 = 0.991) \quad (5)$$

where:

t is the residence time, h

3.3.2 Surface topography

Figure 12 shows the SEM images of peanut shell based biochar prepared under different residence times (1.0, 1.5, 2.0, 2.5, and 3.0 h). As shown in Fig. 12 (a) and (b), when the residence time was 1.0 h or 1.5 h, most of the pores were unformed. As the residence time increased, there were more volatile substances released and more

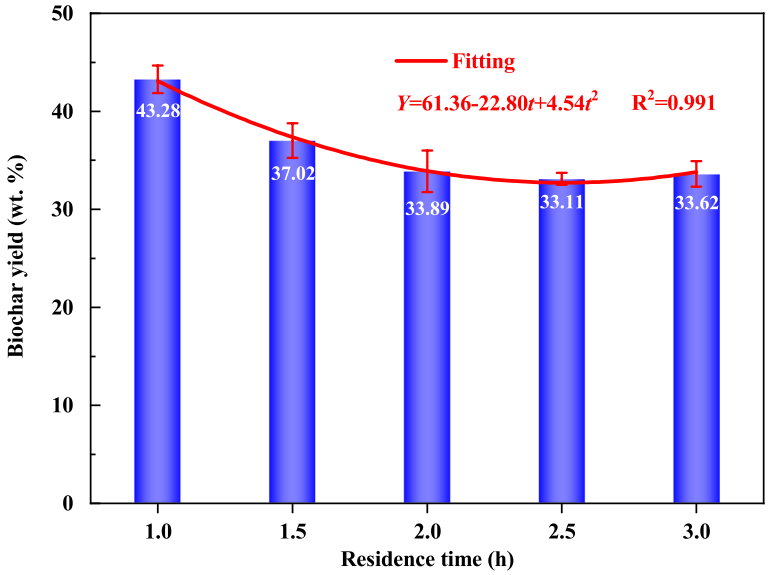

Fig. 11 Biochar yields at different residence times

organic matters such as lignin and cellulose broken down. Thererfore, it can be observed from Fig. 12 (c), (d) and (e) that pore sizes decreased and porosities and pore densities increased with a longer pyrolysis time.

Figure 12 (a) and (b) show the SEM images of biochar prepared at residence time of 1.0 h and 1.5 h, respectively. It could be seen that there were a few pores on the surface of biochar, and most of them were not formed. When the residence time reached 2.5 h or 3.0 h, although the number of pores on the surface of biochar increased compared with that of biochar prepared at the residence time of 1.0 h or 1.5 h, the number of pores on the surface was less than that in Fig. 4(e) (950 °C, 2.0 h, 500 W) or Fig. 8 (e) (800 °C, 2.0 h, 600 W), especially the number of pores with small diameters. In fact, comparing Fig. 4 (e), Fig. 8 (e) and Fig. 12 (e) with Fig. 12(c) (800 °C, 2.0 h, 500 W), it could be found that pyrolysis temperature had the greatest impact on the pore structures of biochar, followed by microwave power, and residence time had the smallest impact.

3.3.3 Pore size distribution

As shown in Fig. 12 (c) and (e), biochar obtained at 3.0 h possessed the higher porosity than the biochar obtained at 2.0 h. The N_2 adsorption–desorption isotherms were obtained to study the pore structure properties of the produced biochars. The DFT method was used to analyze the pore size distribution in the range of 1 ~ 8 nm and the results are shown in Fig. 13. It can be seen that when the residence time was 1.0 h, there were almost no micropores (< 2 nm) in the biochar; when the residence time exceeded 1.5 h, the pore volumes of micropores increased gradually with the increase of time (0.0005 cc/(g·nm) vs 0.015 cc/(g·nm) for 1.0 h vs 3.0 h).

3.3.4 Pore structure parameters

Figure 14 shows the micropore volumes of peanut shell based biochars produced at different residence times (1.0, 1.5, 2.0, 2.5, and 3.0 h). The micropore did not appear until the residence time reached 2.0 h, and with the time extended from 2.0 h to 3.0 h, the micropore volume increased gradually from 0.003 cc/g to 0.005 cc/g. These results largely indicated that with the increase of residence time, the decomposition of biochar is more serious and more volatile substances are released. Therefore, the primary pore structure inside biochar will be improved due to the accelerated release of the volatiles (Lua et al. 2004). At the same time, biochars produced featured a larger micropore volume (0 cc/g vs 0.005 cc/g for 1.0 h vs 3.0 h) with a longer pyrolysis time (Luo et al. 2015).

In this study, a linear equation was given to represent the function correlation between the micropore volume V_{micro} and residence time t:

$$V_{micro} = -1 + 2t(R^2 = 1.000) \quad (6)$$

3.4 Main contribution

In this study, the obtained biochar yield (43.38–30.04 wt. %) was close to the results which were reported by the other researchers for biochars produced by the pyrolysis of peanut shells, i.e., 35.5–42.0 wt. % by Chu et al. (2017), 30.72–41.46 wt. % by Yu et al. (2016), 30–38.3 wt. % by Liu et al. (2022b), 33.6–47.9 wt. % by Shan et al. (2020), 30.00–50.00 wt. % by Rehrah et al. (2014), etc. In this

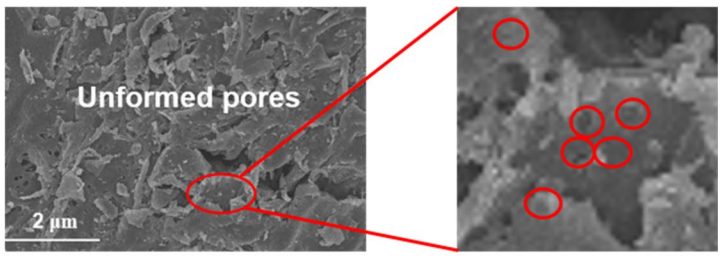

(a) 1.0 h

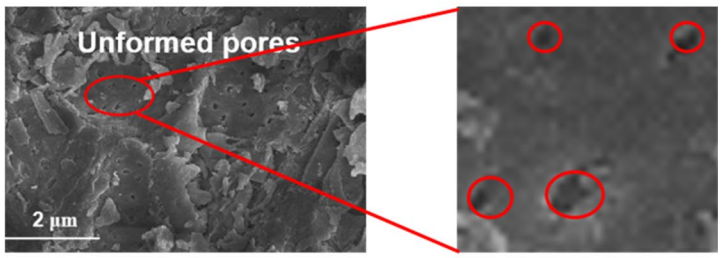

(b) 1.5 h

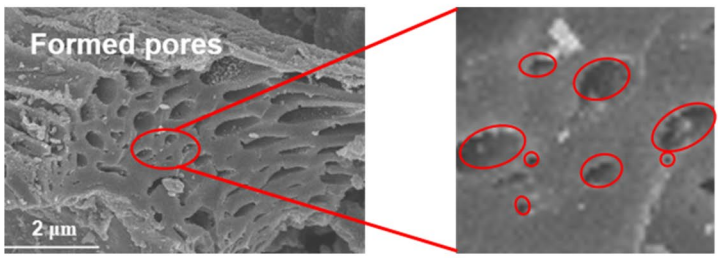

(c) 2.0 h

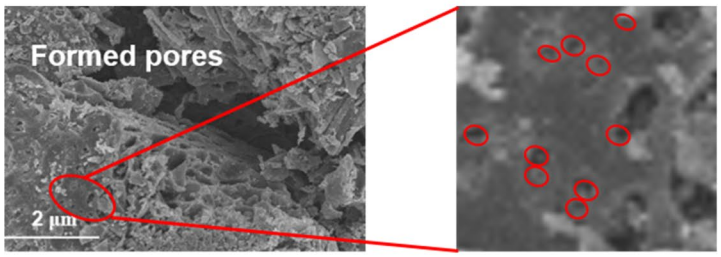

(d) 2.5 h

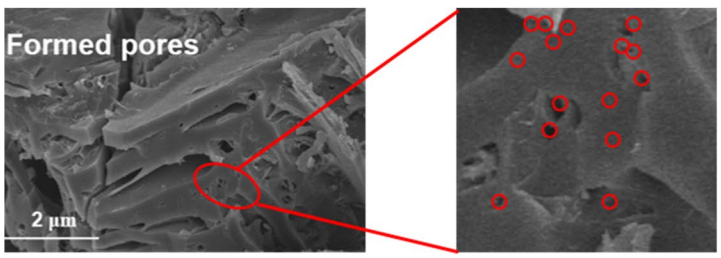

(e) 3.0 h

Fig. 12 SEMs of biochars at different residence times. **a** 1.0 h, **b** 1.5 h, **c** 2.0 h, **d** 2.5 h, **e** 3.0 h

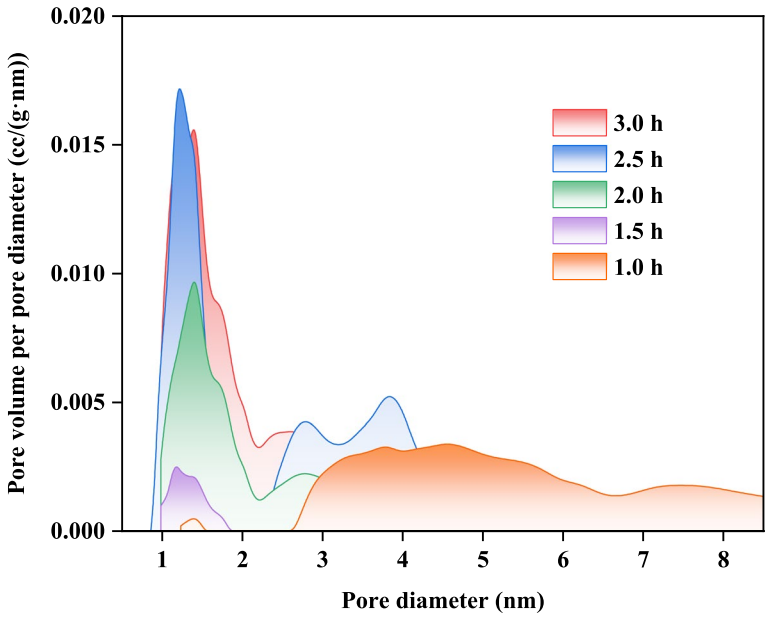

Fig. 13 Pore size distributions of biochars at different residence times

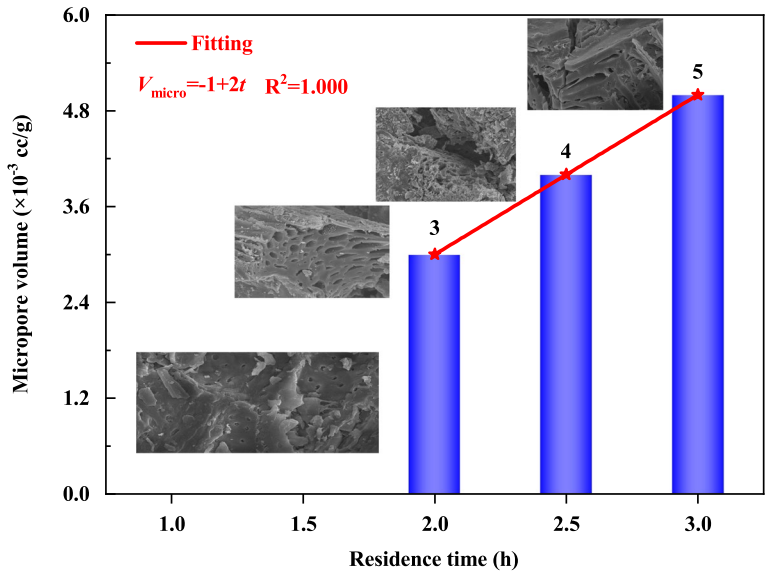

Fig. 14 Micropore volumes of biochars at different residence times

study, the biochar yields decreased monotonously and stabilized around 30 wt. % when the pyrolysis temperature, microwave power, and residence time increased. It also can be found that the left boundaries of the biochar yield ranges in different references were around 30 wt. %. This indicates that when the experimental conditions exceed a certain limit, the biochar yields are determined by the kinds of biomass materials or the ratio of cellulose, hemicellulose and lignin (Antal MJ Jr and Grønli 2003; McHenry 2009).

When the pyrolysis temperature was 950 °C, the microwave power was 500 W, and the residence time was 2.0 h, biochar with the highest specific surface area was obtained in this study and the specific surface area was 67.29 m^2/g. This specific surface area (67.29 m^2/g) was higher than the specific surface area obtained by the

other scholars using conventional electric pyrolysis, i.e., 4.62 m^2/g by Liu et al. (2022b), 6.45 m^2/g by Shan et al. (2020), 20.96 m^2/g by Liu et al. (2018), 23.57 m^2/g by Yu et al. (2016). However, this specific surface area (67.29 m^2/g) was much lower than the specific surface area (587 m^2/g) reported by Chu et al. (2017) for microwave pyrolysis of peanut shell at 600 °C, 2.0 h, 500 W. There are two reasons that could likely explain this phenomenon. The first one is the pyrolysis temperature which has a great effect on the specific surface area. For example, Chu et al. (2017) regarded the temperature of produced gas as the pyrolysis temperature and we detected the temperature of peanut shell and biochar. Actually, when the temperature of produced gas reached 600 °C, the temperature of biochar has exceeded 1000 °C in this study. Another difference was between the pre- and post-treatment. Chu et al. (2017) washed the biochar repeatedly after pyrolysis by deionized water. In this way, ash or tar that may block or destroy the pore structure of biochar would be removed, and the specific surface area increased. Also, peanut shells from different sources influenced the results. The specific surface area of peanut shell used by Li et al. (2020) reached 16.94 m^2/g before pyrolysis, which was higher than 15.88 m^2/g for the specific surface area of biochar obtained in this study at pyrolysis temperature of 750 °C.

Biochar prepared from microwave-assisted pyrolysis has huge application prospects because of the large specific surface area and rich pore structure. Peanut shell based biochar can be used in carbon dioxide capture, hydrogen storage, and catalyst support. The relationship between pore structures and experimental conditions obtained in this study can guide the preparation of biochar with different pore size distributions. These biochars can be used to adsorb gas particles with a specific diameter, such as carbon dioxide, hydrogen and so on. In addition, the biochar can also be used as a catalyst carrier to prepare catalysts by adsorbing some catalyst particles with specific sizes. The larger the pore volume and specific surface area, the larger the adsorption capacity of small molecules by biochar will be.

4 Conclusions

The yields, surface topographies, and pore structures (pore size distribution and micropore volume) of peanut shell based biochars produced at different pyrolysis temperatures (700, 750, 800, 850, 900, and 950 °C), microwave powers (350, 400, 450, 500, and 550 W), and residence times (0.5, 1.0, 1.5, 2.0, and 3.0 h) were explored. Some conclusions were drawn from the research as shown below. Depending on the experimental operating parameters, the yields of biochar were in a range of 30.04–43.38 wt. %. In addition, the yield gradually decreased and finally stabilized with the increases of the pyrolysis temperature, microwave power, or residence time. While the specific surface area improved within the range of 4.68–67.29 m^2/g when there were increases in pyrolysis temperature, microwave power, or residence time. Micropores started to appear at 800 °C, 500 W, and 2.0 h. The maximum specific surface area was 67.29 m^2/g at the reaction parameters of 950 °C, 500 W, and 2.0 h. Because of the large specific surface area, uniform pore structure, and large proportion of microwave volume, the peanut shell based biochar prepared in this study can be used to adsorb gaseous pollutants and organic pollutants in gas or liquid. However, there are still some limitations in this study: a) the maximum specific surface area of biochar was 67.29 m^2/g, which was still smaller than that of activated carbon which is usually several hundred m^2/g; b) more types of characterizations such as XRD, FTIR, EDS can be added to further analyze the properties of peanut shell based biochar; c) In this manuscript, the microwave-assisted pyrolysis of peanut shell and the influence of pyrolysis conditions on the properties of biochar were studied, but the adsorption application of biochar was not paid much attention. Therefore, the following can be done in the future: a) improve the specific surface area of biochar through pretreatment of raw materials or post-treatment of biochar; b) use more types of characterizations to analyze properties of biochar; c) more in-depth "adsorption kinetics" or "adsorption experiments" can be done to evaluate the adsorption capacity of the biochar.

Acknowledgements
The authors thank the National Natural Science Foundation of China (52076049), and Heilongjiang Province "Double First-class" Discipline Collaborative Innovation Achievement Project (LJGXCG2023-080).

Authors' contributions
Tianhao Qiu and Chengxiang Li prepared the original draft; Mengmeng Guang contributed to the conceptualization; and Yaning Zhang supervised the study, and reviewed and edited the article.

Funding
Financial support was provided by the National Natural Science Foundation of China (52076049), and Heilongjiang Province "Double First-class" Discipline Collaborative Innovation Achievement Project (LJGXCG2023-080).

Availability of data and materials
Data will be made available on the reasonable request.

Declarations

Competing interests
The authors declare that they have no known competing financial interests or personal relationships that could have appeared to influence the work reported in this article.

Author details
[1]School of Energy Science and Engineering, Harbin Institute of Technology, Harbin 150001, China. [2]State Key Laboratory of Multiphase Complex Systems, Institute of Process Engineering, Chinese Academy of Sciences, Beijing 100190, China.

Received: 8 October 2023 Revised: 18 October 2023 Accepted: 25 October 2023
Published online: 22 November 2023

References

Açma HH, Meriçboyu AE, Küçükbayrak S. Effect of mineral matter on the reactivity of lignite chars[J]. Energy Conversion & Management, 2001, 42(1), pp: 11–20. https://doi.org/10.1016/s0196-8904(00)00040-6

Ahmad M, Rajapaksha AU, Lim JE, et al. Biochar as a sorbent for contaminant management in soil and water: A review[J]. Chemosphere, 2014, 99, pp: 19–33. https://doi.org/10.1016/j.chemosphere.2013.10.071

Amen R, Bashir H, Bibi I et al (2020) A critical review on arsenic removal from water using biochar-based sorbents: The significance of modification and redox reactions[J]. Chem Eng J 396:125195. https://doi.org/10.1016/j.cej.2020.125195

Antal MJ Jr., Grønli M. The art, science and technology of charcoal production[J]. Industrial & Engineering Chemistry Research, 2003, 42, pp: 1619–1640. https://doi.org/10.1021/ie0207919

Antonangelo JA, Zhang H, Sun X, et al. Physicochemical properties and morphology of biochars as affected by feedstock sources and pyrolysis temperatures[J]. Biochar, 2019, 1, pp: 325–336. https ://doi.org/https://doi.org/10.1007/s42773-019-00028-z

Arpiaa AA, Chen WH, Lam SS, et al. Sustainable biofuel and bioenergy production from biomass waste residues using microwave-assisted heating: A comprehensive review[J]. Chemical Engineering Journal, 2021, 403, pp: 126233. https://doi.org/10.1016/j.cej.2020.126233

Bornemann LC, Kookana RS, Welp G (2007) Differential sorption behaviour of aromatic hydrocarbons on charcoals prepared at different temperatures from grass and wood[J]. Chemosphere 67(5):1033–1042. https://doi.org/10.1016/j.chemosphere.2006.10.052

Chen G, Andries J, Luo Z et al (2003) Biomass pyrolysis/gasification for product gas production: the overall investigation of parametric effects[J]. Energy Convers Manage 44:1875–1884. https://doi.org/10.1016/S0196-8904(02)00188-7

Cheng Q, Huang Q, Khan S et al (2016) Adsorption of Cd by peanut husks and peanut husk biochar from aqueous solutions[J]. Ecol Eng 87:240–245. https://doi.org/10.1016/j.ecoleng.2015.11.045

Chen W, Meng J, Han X, et al. Past, present, and future of biochar[J]. Biochar, 2019, 1, pp: 75–87. https ://doi.org/https://doi.org/10.1007/s42773-019-00008-3

Chen W (2019) Inaugural editorial: pioneering the innovation and exploring the future for biochar technology[J]. Biochar 1:1. https://doi.org/10.1007/s42773-019-00010-9

Chen Y, Yang H, Wang X et al (2011) Biomass-based pyrolytic polygeneration system on cotton stalk pyrolysis: Influence of temperature[J]. Biores Technol 107:411–418. https://doi.org/10.1016/j.biortech.2011.10.074

Chu G, Zhao J, Chen F et al (2017) Physi-chemical and sorption properties of biochars prepared from peanut shell using thermal pyrolysis and microwave irradiation[J]. Environ Pollut 227:372–379. https://doi.org/10.1016/j.envpol.2017.04.067

Chutia RS, Kataki R, Bhaskar T. Characterization of liquid and solid product from pyrolysis of Pongamia glabra deoiled cake[J]. Bioresource Technology, 2014, 165, pp: 336–342. https://doi.org/10.1016/j.biortech.2014.03.118

Demiral D, Eryazıcı A, Şensöz S. Bio-oil production from pyrolysis of corncob (Zea mays L.)[J]. Biomass & Bioenergy, 2012, 36, pp: 43–49. https://doi.org/10.1016/j.biombioe.2011.10.045

Deng Y, Huang Q, Gu W, et al. Application of sludge-based biochar generated by pyrolysis: A mini review[J]. Energy Sources, Part A: Recovery, Utilization, and Environmental Effects, 2020. https://doi.org/10.1080/15567036.2020.1826602

Dissanayake PD, You S, Igalavithana AD, et al. Biochar-based adsorbents for carbon dioxide capture: A critical review[J]. Renewable and Sustainable Energy Reviews, 2020, 119, pp: 109582. https://doi.org/10.1016/j.rser.2019.109582

Fan S, Cui L, Zhang Y et al (2023) Value-added biochar production from microwave pyrolysis of peanut shell[J]. Int J Chem Reactor Eng. https://doi.org/10.1515/ijcre-2023-0005

Fan X, Wang X, Zhao B et al (2022) Sorption mechanisms of diethyl phthalate by nutshell biochar derived at different pyrolysis temperature[J]. J Environ Chem Eng 10:107328. https://doi.org/10.1016/j.jaap.2014.03.008

Fodah AEM, Ghosal MK, Behera D. Studies on microwave-assisted pyrolysis of rice straw using solar photovoltaic power[J]. BioEnergy Research, 2020, 14(1). https://doi.org/10.1007/s12155-020-10172-1

Fodah AEM, Ghosal MK, Behera D. Solar-powered microwave pyrolysis of corn stover for valueadded products and process techno-economic assessment[J]. International Journal of Energy Research, 2020, 23, pp: 1–16. https://doi.org/10.1002/er.6192

Fodah AEM, Ghosal MK, Behera D. Microwave-assisted pyrolysis of agricultural residues: current scenario, challenges, and future direction[J]. International Journal of Environmental Science and Technology, 2021, 3. https://doi.org/10.1007/s13762-020-03099-9

Fodah AEM, Ghosal MK, Behera D. Quality assessment of bio-oil and biochar from microwave-assisted pyrolysis of corn stover using different adsorbents[J]. Journal of the Energy Institute, 2021, 98, pp: 63–76. https://doi.org/10.1016/j.joei.2021.06.008

Fodah AEM, Ghosal MK, Behera D. Bio-oil and biochar from microwave-assisted catalytic pyrolysis of corn stover using sodium carbonate catalyst[J]. Journal of the Energy Institute, 2020, 94, pp: 242–251. https://doi.org/10.1016/j.joei.2020.09.008

Fodah AEM, Abdelwahab TAM (2022) Process optimization and technoeconomic environmental assessment of biofuel produced by solar powered microwave pyrolysis[J]. Sci Rep 12:1–10. https://doi.org/10.1038/s41598-022-16171-w

Ghodszad L, Reyhanitabar A, Maghsoodi MR, et al. Biochar affects the fate of phosphorus in soil and water: A critical review[J]. Chemosphere, 2021, 283, pp: 131176. https://doi.org/10.1016/j.chemosphere.2021.131176

Huang Q, Song S, Chen Z et al (2019) Biochar-based materials and their applications in removal of organic contaminants from wastewater: state-of-the-art review[J]. Biochar 1:45–73. https://doi.org/10.1007/s42773-019-00006-5

Ippolito JA, Cui L, Kammann C et al (2021) Feedstock choice, pyrolysis temperature and type influence biochar characteristics: a comprehensive meta-data analysis review[J]. Biochar 2:421–438. https://doi.org/10.1007/s42773-020-00067-x

Jung K-W, Hwang M-J, Ahn K-H et al (2015) Kinetic study on phosphate removal from aqueous solution by biochar derived from peanut shell as renewable adsorptive media[J]. Int J Environ Sci Technol 12:3363–3372. https://doi.org/10.1007/s13762-015-0766-5

Ke C, Zhang Y, Li B et al (2019) Syngas production from microwave-assisted air gasification of biomass: Part 1 model development[J]. Renewable Energy 140:772–778. https://doi.org/10.1016/j.renene.2019.03.025

Li H, Liu S, Qiu S et al (2020) Catalytic ozonation oxidation of ketoprofen by peanut shell-based biochar: Effects of the pyrolysis temperatures[J]. Environ Technol 43(6):848–860. https://doi.org/10.1080/09593330.2020.1807610

Liu J, Wang H, Ma N et al (2022b) Optimization of the raw materials of biochars for the adsorption of heavy metal ions from aqueous solution[J]. Water Sci Technol 85(10):2869–2881. https://doi.org/10.2166/wst.2022.158

Liu R, Liu G, Yousaf B et al (2018) Operating conditions-induced changes in product yield and characteristics during thermal-conversion of peanut shell to biochar in relation to economic analysis[J]. J Clean Prod 193:479–490. https://doi.org/10.1016/j.jclepro.2018.05.034

Liu Z, Sun Y, Xinrui Xu et al (2020) Preparation, characterization and application of activated carbon from corn cob by KOH activation for removal of Hg(II) from aqueous solution[J]. Biores Technol 306:123154. https://doi.org/10.1016/j.biortech.2020.123154

Liu Z, Ziyi Xu, Linfeng Xu et al (2022a) Modifed biochar: synthesis and mechanism for removal of environmental heavy metals[J]. Carbon Research 1:8. https://doi.org/10.1007/s44246-022-00007-3

Luo L, Chuang Xu, Chen Z et al (2015) Properties of biomass-derived biochars: Combined effects of operating conditions and biomass types[J]. Biores Technol 192:83–89. https://doi.org/10.1016/j.biortech.2015.05.054

Lua AC, Yang T, Guo J. Effects of pyrolysis conditions on the properties of activated carbons prepared from pistachio-nut shells[J]. Journal of Analytical and Applied Pyrolysis, 2004, 72, pp: 279–287. https://doi.org/10.1016/j.jaap.2004.08.001

McHenry MP (2009) Agricultural bio-char production, renewable energy generation and farm carbon sequestration in Western Australia: Certainty, uncertainty and risk[J]. Agr Ecosyst Environ 129(1–3):1–7. https://doi.org/10.1016/j.agee.2008.08.006

Motasemi F, Salema AA, Afzal MT. Dielectric characterization of corn stover for microwave processing technology[J]. Fuel Processing Technology, 2015, 131, pp: 370–375. https://doi.org/10.1016/j.fuproc.2014.12.006
Motasemi F, Afzal MT. A review on the microwave-assisted pyrolysis technique[J]. Renewable and Sustainable Energy Reviews, 2013, 28, pp: 317–330. https://doi.org/10.1016/j.rser.2013.08.008
Nguyen VT, Nguyen TMT, Liu YG, et al. Fabrication of partially graphitic biochar for the removal of diclofenac and ibuprofen from aqueous solution: Laboratory conditions and real sample applications[J]. Environmental Engineering Science, 2021, 38(10), pp: 974–989. https://doi.org/10.1089/ees.2020.0202
Novak JM, Ippolito JA, Watts DW et al (2019) Biochar compost blends facilitates switchgrass growth in mine soils by reducing Cd and Zn bioavailability[J]. Biochar 1:97–114. https://doi.org/10.1007/s42773-019-00004-7
Özçimen D, Ersoy-Meriçboyu A (2010) Characterization of biochar and bio-oil samples obtained from carbonization of various biomass materials[J]. Renewable Energy 35(6):1319–1324. https://doi.org/10.1016/j.renene.2009.11.042
Palansooriya KN, Wong JTF, Hashimoto Y, et al. Response of microbial communities to biochar-amended soils: a critical review. Biochar. 2019;1, pp: 3–22. https://doi.org/10.1007/s42773-019-00009-2
Qiao Yu, Zhang C, Kong F et al (2021) Activated biochar derived from peanut shells as the electrode materials with excellent performance in Zinc-air battery and supercapacitance[J]. Waste Manage 125:257–267. https://doi.org/10.1016/j.wasman.2021.02.057
Qiuhao Wu, Wang Y, Jiang L et al (2019) Microwave-assisted catalytic upgrading of co-pyrolysis vapor using HZSM-5 and MCM-41 for bio-oil production: Co-feeding of soapstock and straw in a downdraft reactor[J]. Biores Technol 299:122611. https://doi.org/10.1016/j.biortech.2019.122611
Rehrah D, Reddy MR, Novak JM et al (2014) Production and characterization of biochars from agricultural by-products for use in soil quality enhancement[J]. J Anal Appl Pyrol 108:301–309. https://doi.org/10.1016/j.jaap.2014.03.008
Reza MdS, Afroze S, Bakar MSA, et al. Biochar characterization of invasive Pennisetum purpureum grass: effect of pyrolysis temperature[J]. Biochar, 2020, 2, pp: 239–251. https://doi.org/10.1007/s42773-020-00048-0
Shan R, Shi Y, Jing Gu et al (2020) Single and competitive adsorption affinity of heavy metals toward peanut shell-derived biochar and its mechanisms in aqueous systems[J]. Chin J Chem Eng 28:1375–1383. https://doi.org/10.1016/j.cjche.2020.02.012
Sun Y, Zhang Z, Sun Y, et al. One-pot pyrolysis route to Fe—N-Doped carbon nanosheets with outstanding electrochemical performance as cathode materials for microbial fuel cell[J]. International Journal of Agricultural and Biological Engineering, 2020, 13(6), pp: 207–214. https://doi.org/10.25165/j.ijabe.20201306.5765
Tayibi S, Monlau F, Fayoud NE, et al. One-pot activation and pyrolysis of Moroccan Gelidium sesquipedale red macroalgae residue: production of an efficient adsorbent biochar. Biochar. 2019 1, pp: 401–412. https://doi.org/10.1007/s42773-019-00033-2
Tripathi M, Sahu JN, Ganesan P. Effect of process parameters on production of biochar from biomass waste through pyrolysis: A review[J]. Renewable and Sustainable Energy Reviews, 2016, 55, pp: 467–481. https://doi.org/10.1016/j.rser.2015.10.122
Wang Y, Ke L, Peng Y et al (2020a) Ex-situ catalytic fast pyrolysis of soapstock for aromatic oil over microwave-driven HZSM-5@SiC ceramic foam[J]. Chem Eng J 402:126239. https://doi.org/10.1016/j.cej.2020.126239
Wei X, Xue X, Liu Wu et al (2020) High-grade bio-oil produced from coconut shell: A comparative study of microwave reactor and core-shell catalyst[J]. Energy 212:118692. https://doi.org/10.1016/j.energy.2020.118692
Wang P, Liu X, Bochi Yu et al (2020b) Characterization of peanut-shell biochar and the mechanisms underlying its sorption for atrazine and nicosulfuron in aqueous solution[J]. Sci Total Environ 702:134767. https://doi.org/10.1016/j.scitotenv.2019.134767
Wu P, Ata-Ul-Karim ST, Singh BP, et al. A scientometric review of biochar research in the past 20 years (1998–2018) [J]. Biochar, 2019, 1, pp: 23–43. https://doi.org/10.1007/s42773-019-00002-9
Yu P, Xue Y, Gao F et al (2016) Phosphorus removal from aqueous solution by pre- or post-modified biochars derived from agricultural residues[J]. Water Air Soil Pollut 227:370. https://doi.org/10.1007/s11270-016-3066-x
Zhang P, Sun H, Li Yu et al (2013) Adsorption and catalytic hydrolysis of carbaryl and atrazine on pig manure-derived biochars: Impact of structural properties of biochars[J]. J Hazard Mater 244–245:217–224. https://doi.org/10.1016/j.jhazmat.2012.11.046
Zhang T, Mao J, Liu X et al (2017a) Pinecone biomass-derived hard carbon anodes for high-performance sodium-ion batteries[J]. RSC Adv 7:41504–41511. https://doi.org/10.1039/c7ra07231g
Zhang X, Sunb P, Wei K et al (2020c) Enhanced H_2O_2 activation and sulfamethoxazole degradation by Fe-impregnated biochar[J]. Chem Eng J 385:123921. https://doi.org/10.1016/j.cej.2019.123921
Zhang Xu, Yao H, Lei X et al (2021) Synergistic adsorption and degradation of sulfamethoxazole from synthetic urine by hickory-sawdust-derived biochar: The critical role of the aromatic structure[J]. J Hazard Mater 418:126366. https://doi.org/10.1016/j.jhazmat.2021.126366
Zhang Y, Fan S, Liu T et al (2022) A review of biochar prepared by microwave-assisted pyrolysis of organic wastes[J]. Sustainable Energy Technol Assess 50:101873. https://doi.org/10.1016/j.seta.2021.101873
Zhang Y, Ke C, Wenming Fu et al (2020b) Simulation of microwave-assisted gasification of biomass: A review[J]. Renewable Energy 154:488–496. https://doi.org/10.1016/j.renene.2020.03.056
Zhang Y, Zhang J, Chen F, et al. Influence of biochar with loaded metal salts on the cracking of pyrolysis volatiles from corn straw[J]. Energy Sources, Part A: Recovery, Utilization, and Environmental Effects, 2020. https://doi.org/10.1080/15567036.2020.1779414
Zhang Yu, Jiaqiang Wang Xu, Bian, et al (2017b) A continuous gas leakage localization method based on an improved beamforming algorithm[J]. Measurement 106:143–151. https://doi.org/10.1016/j.measurement.2017.04.030

Publisher's Note